Journal of Medicinal and Chemical Sciences 7 (2024) 753-776

Journal of Medicinal and Chemical Sciences

Journal homepage: http://www.jmchemsci.com/

Original Article

Formulation and Development of Doxycycline Hyclate Loaded Chitosan Nanoparticles Crosslinked Topical Hydrogel Patches for Healing Diabetic Foot Ulcer

Sidhavatam Harshavardhan Reddy, Manimaran V*

Department of Pharmaceutics, SRM College of Pharmacy, SRM Institute of Science and Technology, Kattankulathur, Chengalpattu, Tamil Nadu 603203, India

ARTICLEINFO

Article history

Submitted: 2024-01-06
Revised: 2024-03-26
Accepted: 2024-04-03
ID: JMCS-2403-2471
Checked for Plagiarism: **Yes**
Language Editor Checked: **Yes**

DOI:10.26655/JMCHEMSCI.2024.6.1

KEYWORDS

Diabetic foot ulcer
Doxycycline hyclate
Chitosan nanoparticles
Franz diffusion
Polymeric matrix
Topical hydrogel patches

ABSTRACT

Diabetic foot ulcer pose a significant challenge in healthcare, often leading to prolonged healing processes and complications requiring sophisticated and advanced therapeutic interventions. This study focuses on the formulation and development of Doxycycline hyclate loaded chitosan nanoparticles in cross-linked topical hydrogel patches for targeted management of DFU healing. Various characterization techniques, such as FT-IR, Zeta potential, DSC, XRD, and SEM, were employed to confirm and gain insights into the structural and morphological features of the cross-linked topical hydrogel patches. The evaluation parameters encompassed analyzing sol-gel behavior, swelling dynamics, and *in vitro* drug release studies at pH values of 5.5, 6.5, and 7.4. Drug permeation and deposition was performed utilizing the Franz diffusion cell method. The topical hydrogel patches showed pH-sensitive behavior, with enhanced drug release, swelling, and permeation observed at pH 7.4. The synthesized nanoparticles exhibited a spherical morphology, varying particle sizes ranging from 92.83 nm to 206.2 nm, and a zeta potential measuring -22.4 mV. The patches were produced by incorporating CNPs as carriers for DCH into a polymeric matrix, which required the optimization of free radical polymerization. The ion gelation method was utilized to prepare the CNPs. The solvent evaporation technique was used for grafting the topical hydrogel patches. Among the seven formulations, topical hydrogel patch F6 exhibited the most favorable characteristics, as evidenced by a substantial drug content of 97.21 ± 0.524%. The F6 formulation excelled over other formulations over 72 hours at pH 7.4. Stability testing of the selected F6 formulation over 6 months under accelerated conditions confirmed its viability. Therefore, this polymeric network represents an innovative technology for accelerating the healing process of diabetic foot ulcers through the use of doxycycline hyclate loaded chitosan nanoparticles cross-linked in topical hydrogel patches.

GRAPHICAL ABSTRACT

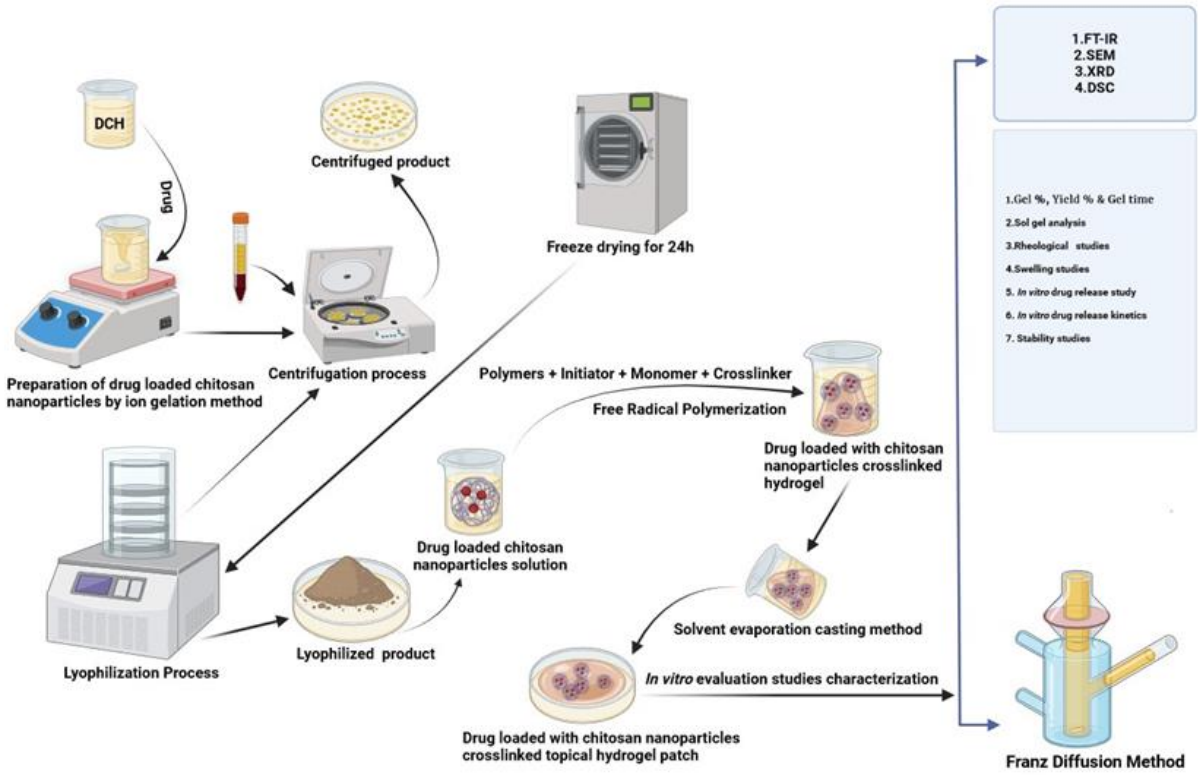

Introduction

Diabetic foot ulcer (DFU) is debilitating complications of diabetes mellitus, resulting from a combination of neuropathy and impaired blood flow. These ulcers often resist conventional healing processes, leading to chronic wounds that are highly susceptible to infections [1]. If left untreated, DFU can progress to severe complications, including tissue necrosis and limb amputation. The prognosis for DFU healing varies based on factors like the size and depth of the ulcer, the presence of infections, and the treatment effectiveness [2]. Globally, the burden of diabetes and its complications is substantial. In 2022, approximately 492 million people were living with diabetes, and projections estimate a 68.2% increase by 2045. The DFU prevalence among diabetic individuals ranges from 15% to 30%. These statistics underscore the urgent need for effective and innovative therapeutic strategies to address the growing challenge of DFU on a global scale [3]. The primary goals of treatment are to facilitate wound closure, prevent infection, address underlying causes such as peripheral neuropathy and vascular insufficiency, and ultimately restore functionality to the affected limb. Wound care typically involves regular debridement to remove dead or infected tissue, offloading pressure from the affected area to promote healing, and managing any underlying infections [4]. Advanced wound dressings, topical antimicrobial agents, and, in some cases, surgical interventions may be employed to optimize the healing process. In addition, maintaining glycemic control is crucial for promoting overall wound healing in individuals with diabetes [5]. This study aims to show that Doxycycline hyclate (DCH) loaded chitosan nanoparticles (CNPs) cross-linked hydrogel patches have emerged as a promising therapeutic strategy for managing DFU, particularly those complicated by bacterial infections. These hydrogel patches offer a versatile platform for localized drug delivery, creating a conducive environment for wound healing [6].

The polymeric matrix provides mechanical support, while the hydrogel structure ensures moisture retention, facilitating optimal conditions for tissue regeneration. In the pursuit of an effective and targeted treatment, DCH has been incorporated into CNPs cross-linked hydrogel patches, utilizing CNPs as a carrier. Chitosan, derived from crustacean exoskeletons, serves as an excellent polymeric matrix due to its biocompatibility and biodegradability [7]. The ion gelation process is employed to create a cross-linked hydrogel structure, involving the CNPs interaction with carbopol 934 and additional components such as Hydroxypropylmethylcellulose (HPMC), Tween 80, Dimethyl sulfoxide (DMSO), PEG-10000, Ammonium Persulfate (APS), Acrylic Acid (AA), and Methylenebisacrylamide (MBA). DCH is a broad-spectrum antibiotic known for its efficacy against various bacterial pathogens. In the context of DFU management, DCH plays a crucial role in preventing and treating infections that can accelerate the healing process [8]. The ion gelation process involves the crosslinking of CNPs by carbopol 934 as a crosslinking agent. This results in the formation of a three-dimensional hydrogel structure. The inclusion of Tween 80 enhances the stability and solubility of DCH within the hydrogel, while PEG 10000 contributes to the mechanical strength. HPMC is a film-forming agent and also gives gel strength [9]. DMSO aids in dissolving and incorporating the components, ensuring uniform drug distribution. APS, AA, and MBA are critical components in the crosslinking process, determining the hydrogel's structure and drug release kinetics. The formulation of CNPs cross-linked hydrogel patches incorporating DCH and CNPs presents a rational approach to DFU treatment. The ion gelation process allows for the precise control of the hydrogel's physical and chemical properties, ensuring optimal drug release kinetics [10]. Chitosan's biocompatibility and biodegradability contribute to the safety of the formulation. The additional components, including carbopol 934, HPMC, Tween 80, DMSO, PEG-10000, APS, AA, and MBA, are carefully selected to achieve a balance between mechanical strength, drug release profile, and overall therapeutic efficacy [11].

This innovative approach not only addresses the challenges of DFU management, but also holds the potential to improve patient outcomes by providing targeted and sustained delivery of antibacterial agents. The development of CNPs cross-linked hydrogel patches incorporating DCH represents a step forward in personalized and effective treatment strategies for diabetic foot ulcers, aiming to enhance foot ulcer healing and mitigate complications associated with these challenging conditions [12].

Materials and Methods

Materials

Doxycycline hyclate was obtained as a gift sample from Spansules Pharmatech Pvt. Ltd., located in Hyderabad, India. Chitosan (Low MW) in its extra-pure form, with a viscosity range of 10-20 mPas and a 90% deacetylation degree, was obtained from Sisco Research Laboratories Pvt. Ltd. in Maharashtra, India. Sodium tripolyphosphate and PEG 10000 were acquired from Sigma Aldrich. Carbopol 934 was sourced from Oryn Healthcare LLP in Ahmedabad, India. Ammonium persulfate was procured from Vizag Chemical, Visakhapatnam, India.

Ethanol was purchased from SR Enterprises in Mumbai, India. Hydroxypropylmethylcellulose and N-Methylenebisacrylamide were sourced from Banner Enterprise in Rafaleshwar, Morbi, Gujarat, India. Tween 80 was obtained from Multichem, Pvt. Ltd., Hyderabad, India. Potassium dihydrogen phosphate, sodium hydroxide, and hydrochloric acid were procured from Annexe Chem Pvt. Ltd., Vadodara, India.

Compatibility study (drug and excipients)

A compatibility analysis is conducted to evaluate the interaction between a drug and its excipients. In the case of DCH, the active pharmaceutical ingredients are combined with polymers in a 100:1 ratio, and this mixture is integrated into pellets using IR-grade KBr. The pellets are formed by applying pressure to a hydraulic press [13]. Subsequently, a Shimadzu FT-IR analyser is employed to examine the pellets, with the

spectrum wavelength ranging from 4500 cm1 to 400 cm^{-1}. This analytical method is instrumental in understanding the compatibility of the drug with various components. The outcome of a drug excipient compatibility study can provide insights into formulation development, stability, safety, efficacy, and bioavailability of the drug product [14].

Determination of absorption maxima (Drug Content)

The assessment of the maximum wavelength, at which a molecule exhibits the strongest light absorption, is a critical parameter in various analytical techniques, including UV-Vis spectroscopy. This characteristic is essential for the identification and quantification of the molecule. Utilizing 7.4 phosphate buffer, standard drug solutions containing 20 mg/ml of DCH were appropriately diluted before undergoing individual in the 200-400nm range [15]. This scanning process aimed to pinpoint the wavelength at which the molecule absorbs light most intensely. The analysis revealed that the maximum absorption for DCH occurred at 272 nm. Therefore, superimposing the spectra of the drug elucidates the point of the maximum absorption [16].

Preparation of DCH incorporating chitosan nanoparticles through Ion gelation technique

In the preparation of a DCH hydrogel patch loaded with CNPs via the ion gelation method, CNPs are initially synthesized by dissolving chitosan in acetic acid, followed by dropwise addition to a sodium tripolyphosphate (STPP) solution. The resulting ion gelation induces the formation of CNPs, which are subsequently loaded with DCH by mixing with a DCH solution in ethanol [14]. The drug-loaded CNPs are then incorporated into a hydrogel-forming material, such as carbopol 934, and stirred until uniform dispersion is achieved. This mixture is applied to a patch substrate, and the hydrogel patch is allowed to form through crosslinking. The hydrogel patch is evaluated for drug loading, particle size, and release kinetics, ensuring optimal properties for controlled drug delivery through the skin. This comprehensive procedure integrates CNPs synthesis, drug loading, and hydrogel patch formation for potential transdermal applications [17].

Investigation of formulated nanoparticles

The determination of the zeta potential and particle size of CNPs was carried out using the ZetaSizer Mastersizer 2000 from Malvern Instruments, UK. The morphological characteristics of the CNPs were examined through scanning electron microscopy at Tescan, UK. Additionally, an investigation was conducted to analyze the drug loaded onto the CNPs using FT-IR spectroscopy [16]. The analysis was performed using a Shimadzu FT-IR Tracer-100 instrument from Japan, with KBr pellets used as the sample preparation method. This method enabled the characterization of the interactions between the drugs and the CNPs, providing valuable insights into the structural changes and chemical bonds involved in the drug loading process [18].

Fabrication of polymeric nanoparticles cross-linked hydrogel patches

The free radical polymerization approach was optimized to formulate topical hydrogel patches containing CNPs cross-linked with the drug. The patches were developed using carbopol 934 and PEG-10000 as the polymers, along with Tween 80 as the surfactant [17]. An individual amount of solutions was prepared with specified quantities of polymer, penetration enhancer, surfactant, APS as the initiator, HPMC as the film-forming agent and gelling property, and MBA as the cross-linker, which is used mostly to maintain the compact structure of the formulation. The monomer acrylic acid, DMSO, was measured separately [19]. Acrylic acid is commonly used in the formulation of hydrogels that have a significant swelling property. DMSO is used to enhance drug penetration. The solutions of carbopol 934, HPMC, tween 80, acrylic acid, APS, and cross-linker were added and incorporated into the polymer solution gradually. The resultant mixture was then poured into Petri dishes that were labeled, covered with aluminum foil, and

placed in a preheated water bath at 50 °C for 2 hours, followed by 60 °C for 24 hrs. Afterwards, the Petri dishes were removed from the water bath, and the prepared patches were cleansed using a water-ethanol solution of 70:30 to remove the impurities and non-reactive compounds. The patches were dried in an oven at 40 °C for two days. After drying, the polymer patches were placed in airtight containers to undergo further testing and analysis [20]. A total of seven different formulations were developed, and the particular contents of each formulation are indicated in Table 1.

Table 1: Formulation composition of hydrogel patches

Formulation code	Drug DCH (mg)	Chitosan:STTP	Carbopol 934 (mg)	HPMC (mg)	Tween 80 (wt.%)	DMSO (wt. %)	PEG 10000 (mg)	APS (mg)	AA (mg)	MBA (mg)
F1	30	2:1	100	25	0.02	0.01	90	82	60	100
F2	30	2:1	100	34	0.01	0.01	95	77	65	90
F3	30	2:1	100	30	0.01	0.02	80	75	70	85
F4	30	2:1	100	27	0.02	0.01	100	85	60	100
F5	30	2:1	100	30	0.01	0.02	95	73	65	95
F6	30	2:1	100	32	0.02	0.01	100	90	75	100
F7	30	2:1	100	28	0.01	0.02	85	80	70	90

Characterization of formulated hydrogel patches

Weight variation and thickness

The weight variation and the thickness of the patch are important quality attributes that need to be controlled to ensure consistent drug delivery and adhesion properties [18]. In this method, three patches from each formulation were weighed and the mean value determined, and a micrometer screw gauge was used to measure the film thickness at three distinct ranges. Following that, each patch was weighed separately on an electronic scale. The patch thickness was measured using vernier calipers and reported [21].

Folding endurance

The evaluation of topical hydrogel patches was done manually, with individual patches being folded repeatedly at the same time until they broke or the development of visible cracks occurred. This approach was deemed suitable for gauging the quality of the patches, serving as a practical measure of their durability [17, 19]. The sample's ability was determined to endure folding, which indicates brittleness. To determine the value of folding endurance and to evaluate the films, it was necessary to count the number of times that the films could be folded in the same spot without encountering any breakage [22].

Gel fraction test

The determination of the gel fraction in blank gels and DCH loaded CNPs cross-linked hydrogel patches involved a process where the gels were dried for 24 hours in an oven set at 50 °C. After the drying period, the gels were weighed, and then immersed in distilled water for 24 hours. Following this duration of immersion, the leftover insoluble gel was subjected to drying in the oven, and then it was weighed again [23].

$$\text{Gelfraction \%} = \frac{We}{Wo} \times 100$$

The gel fraction percentage (%) was determined using Equation (1), with "We" representing the weight of the dry gel insoluble and "W0" indicating the initial polymer weight.

PH Measurement

The pH measurement values of the blank gel and DCH loaded CNPs cross-linked topical hydrogel patches were determined at room temperature 25 °C using a pH metre (Oakton pH 700 Benchtop Metre, Cole-Palmer India Pvt. Ltd., Mumbai). The measurement was performed three times, and

the calibrated electrode tip was submerged directly into the hydrogel [20, 21].

Spreadability study

The spreadability of the hydrogel was measured using the glass slide technique, and two glass slides were taken. A 1 cm circle was drawn in the center of the glass slide, and 0.5 g of gel was placed. The second glass slide was placed on top of the first one, with the hydrogel layered between the two glass slides. A weight of 500g was kept on the top plate for 5 minutes. After 5 minutes, the weight was removed, and the increase in diameter was measured. The results were evaluated based on the extent of the area covered and the amount of mass applied using the given equation [24].

Viscosity study

The viscosity measurements of blank gel and DCH loaded CNPs cross-linked topical hydrogel patches were conducted at room temperature 25 °C using the Instrument of Gel Timer DV2T, AMETEK Brookfield, USA. Formulation F1-F7 was measured using spindle No. 7 [25].

Swelling study

The hydrogel patches that were being studied were tested for their swelling behavior using phosphate buffers with pH levels of 5.5, 6.5, and 7.4. Initially, the topical hydrogel patches were measured and immersed into the corresponding buffer solutions for 36 hours at room temperature [22]. At regular intervals, the patches were removed from the buffer solutions, any excess water was blotted off, and the patches were weighed again using an analytical scale. The topical hydrogel patches were then submerged in the appropriate buffer solutions once again, and the experiment was repeated until a consistent weight was reached [26].

$$\% \text{ swelling} = \frac{(M1 - M0)}{M0} \times 100$$

Rheological study

The rheological characteristics of hydrogel patches were explored using a Brookfield viscometer under room temperature conditions of 25 °C. The assessment involved a stepwise evaluation of hydrogel patches at rotating rpms of 5, 10, 20, 50, and 100. F1 to F7 formulations were measured and evaluated using spindle No. 7 [27].

Gel Strength study

The determination of gel strength in hydrogel patches was conducted through the frequency sweep method employing an RM200 PLUS rheometer (Mauritius Ltd., UK) at 37 °C. In summary, a 1% strain was used in the investigation throughout a frequency range of 0.05-10 Hz [25]. In summary, an investigation was carried out by applying a strain constant of 1% over the frequency spectrum ranging from 0.05 to 10 Hz. After that, the gel strength of the topical hydrogel patches was calculated as the ratio of the storage modulus (G) to the loss modulus (G) [28].

Wettability test

The evaluation of the wettability test for topical hydrogel patches was carried out at room temperature 25 °C. To summarize, 0.2 g of the formulated DCH-loaded CNPs cross-linked topical hydrogel patches were placed on a glass slide [26]. Methylene blue was applied gently to the surface of the DCH-loaded CNPs cross-linked topical hydrogel patches. Digital measurements were conducted to determine the contact angle (ɵ) and the minimum time required for full droplet absorption [29].

Sol-gel analysis of hydrogel patch

The sol-gel analysis method is used to determine the percentage of polymer that remains separate inside the structure of the topical hydrogel formulation. Initially, the topical hydrogel patches underwent a drying process and were carefully weighed (mc) [30]. Consequently, these patches were submerged in distilled water for a week, with intermittent shaking to separate the uncross-linked polymer content from the gel in the hydrogel process. Following this immersion, the patches were carefully placed in per-labeled tripper plates and dried in a vacuum oven at 60

°C. The drying process proceeded until a consistent weight (md) was attained [31].

The sol% (sol fraction) and gel% (gel fraction) were then calculated using the following equation:

$$\text{Sol \%} = 100 - \text{Gel\%}$$

$$\text{Gel \%} = \frac{\text{Md}}{\text{Mc}} \times 100$$

These calculations offered thorough insights into the degree of crosslinking inside the hydrogel structure, allowing for a more in-depth understanding of the composition and characteristics of the formulated topical hydrogel patches.

FT-IR spectroscopy

FT-IR investigations were utilized to explore the interactions that occurred between several distinct moieties, such as the drug, polymer, surfactant, monomer, permeation enhancer, and cross-linker. The investigation relies on the fundamental principle that distinct frequencies of infrared light absorption occur within the chemical bonds of a substance [27]. The samples were finely pulverized to attain a reduced particle size for the analysis. Using a spatula, the resultant substance was subsequently applied to the crystal location to capture the corresponding absorption spectra. The spectra were measured in the frequency range of 4500-400 cm^{-1}. This comprehensive approach allowed for the examination of chemical bonding interactions within the components under investigation [32].

Scanning electron microscopy (SEM)

SEM played a pivotal role in measuring intricate details of the morphological characteristics and performing a complete structural study of the developed topical hydrogel patches. The topical hydrogel patches were meticulously dried, followed by crushing. Subsequently, a part of the dried and crushed patches was carefully positioned on an aluminum stub coated with a thin coating of sputter gold [26]. SEM was utilized to deliver a precisely focused beam of electrons onto the sample, resulting in images that not only provided detailed insights, but also contributed to a thorough and comprehensive understanding of the structural morphology exhibited by the patches. This approach enabled a detailed investigation, shedding light on the intricate details and distinguishing characteristics and features present in the topical hydrogel patches with their structural composition [33].

X-ray diffraction (XRD)

XRD is a sophisticated technique that provides precise information on the unit cell dimensions of materials in both crystalline and amorphous states. XRD was used extensively to examine and characterize the crystallinity of the topical hydrogel patches. The method involved extensive preparation, starting with meticulously crushing the material to attain a fine particle composition [29, 30]. This was followed by a process of homogenization, ensuring uniformity in the sample structure. The prepared samples were then meticulously placed into a plastic sample holder integrated into the XRD instrument. The resulting diffraction pattern generated by a sample material was meticulously captured, documented, and thoroughly analyzed. This analytical procedure not only captured the essence of crystallinity inside the cross-linked topical hydrogel patch, but also provided comprehensive, intricate insights into its structural properties, revealing subtle information about its crystalline nature. The XRD utilization thus emerged as a crucial methodology, providing a comprehensive understanding of the internal structure composition and crystalline features inherent in the topical hydrogel patches under assessment [34].

DSC-Differential scanning calorimetry

DSC was employed to evaluate and determine the transition temperature of the optimized formulation of the topical hydrogel patch. The samples, which ranged from 0.5 mg to 3 mg, were precisely weighed and carefully placed into an aluminum pan. These samples underwent rigorous treatment in the presence of nitrogen gas, encompassing temperatures ranging from 20

to 600 °C while maintaining a constant heating rate of 20 °C per minute [28]. The comprehensive analysis was carried out with accuracy, and the resultant findings were meticulously documented for further investigation. This method allowed for a thorough exploration of the thermal characteristics and transition temperature profile inherent in the optimized topical hydrogel patch formulation [35].

Drug-loading study of formulation

Doxycycline hyclate was incorporated into the topical hydrogel patches in a precise manner. Initially, a 1% concentration of the drug was meticulously mixed with a 0.1 M HCl solution until a clear and uniform solution was achieved. Following that, the dried topical hydrogel patches were then precisely weighed to determine their initial weight. Subsequently, these pre-weighed topical hydrogel patches were immersed in the DCH solution for 24 hours while kept at room temperature [32, 33].

After the specified immersion, the drug-loaded topical hydrogel patches were carefully removed from the solution. To ensure the elimination of any excess solution contents that remained on the patch surface, a thorough wash with distilled water was carried out. Following the washing stage, the patches were dried in a vacuum oven set at 40 °C. After the drying process was complete, the patches were weighed again to determine the final weight. The quantity of drug placed in the hydrogel patches was then precisely calculated using a predetermined equation, allowing for an exact measurement of the drug content inside the formulated topical hydrogel patches. This comprehensive procedure required the precise incorporation of the desired drug quantity into the hydrogel matrix, resulting in effective drug delivery and therapeutic efficiency [36].

$$\text{Percent drug loading} = \frac{\text{Final weight of topical hydrogel patch} - \text{Initial weight of topical hydrogel patch}}{\text{Total drug used in loading}} \times 100$$

$$\text{Entrapment Efficiency (\%)} = \frac{\text{Actual drug contents in topical hydrogel patch}}{\text{Theoretical drug contents in topical hydrogel patch}} \times 100$$

In vitro drug release study of hydrogel patch

The *in vitro* release study of topical hydrogel patches was thoroughly investigated across pH levels of 5.5, 6.5, and 7.4. The regulated, controlled drug release mechanism was conducted using a USP-II dissolution apparatus. Phosphate buffer solutions, adjusted to precise pH values, were meticulously prepared and placed into the dissolution apparatus vessels, with a total volume of 500 mL each. The temperature was precisely maintained at a consistent 37±0.5 °C, and the paddle speed was stirred at 50 rpm. After precisely weighing the drug-loaded topical hydrogel patches, they were accurately weighed and submerged into the vessels filled with buffer [35]. At specified intervals, samples were precisely withdrawn using a pipette at predetermined intervals, and the conditions were maintained by quickly adding solution in dissolution media. The samples that were withdrawn underwent filtration and dilution with a fresh buffer solution before being analyzed for drug release using a UV-Vis spectrophotometer at 272 nm. Following that, the drug release kinetics from the developed formulations was modeled according to the five distinct kinetic models: zero-order, first-order, Korsmeyer Peppas, Higuchi, and Hixson Crowell. The release kinetics of polymer-loaded hydrogel patches were determined to be most accurately explained by the release kinetic model with the highest coefficient of determination R^2 value [37].

In vitro drug release study through franz diffusion cell

The Franz diffusion cell was utilized to evaluate the drug deposition profile that was observed over a synthetic membrane. The *ex vivo* evaluation of drug-loaded chitosan nanoparticle cross-linked hydrogel patches was evaluated at three different pH levels: 5.5, 6.5, and 7.4. During the experiment, the phosphate buffer was kept at

a constant temperature of 32±0.5 °C inside the diffusion cell, and the receptor compartment was continuously stirred. This was done to ensure that the phosphate buffer was maintained at each pH level [32]. A cellophane membrane with a pore size of 0.45 µm was used to distinguish the donor compartment from the receptor compartment. A sample of the formulated topical hydrogel patch was then placed in the donor compartment and placed over the synthetic membrane [35]. The patch had an area of 1.5 cm^2. At predetermined intervals, 1 mL of samples was withdrawn from the diffusion cell, and the fresh medium was replenished each time. After the samples were withdrawn, they were diluted with the medium, and then they were analyzed using a UV-Vis spectrophotometer at a wavelength of 272 nm [38].

Stability studies

According to ICH guidelines, stability studies are carried out to evaluate the formulation of DCH loaded CNPs cross-linked in topical hydrogel patches' ability to maintain drug content over an extended period under various storage conditions. Samples were stored in stability chambers for six months at different RHs and conditions. The stored RH/conditions were 25±0.5 °C & 60±5% RH, 30±0.5 °C & 65±5% RH, 30±0.5 °C & 75±5% RH, and 40±0.5 °C & 75±5%. At 1, 2, 3, and 6 months, samples were withdrawn for analysis of drug content [39].

Results and Discussion

Drug excipients and compatibility study

The FT-IR spectra of pure DCH, along with those of polymers, are presented in and Table 2 and Figure 1. The FT-IR spectra obtained for the physical mixtures reveal distinct peaks associated with DCH, indicating compatibility with the polymers within the matrix. This result provides additional evidence that the chemical integrity of the specific drugs remains unaltered during the formulation process. Further confirmation of compatibility between DCH and the hydrogel patch formulation F6 is displayed in Figure 1, where the FT-IR spectra of DCH show no additional indications of drug incompatibility with the polymer. This meticulous analysis underscores the careful consideration given to ensuring the chemical harmony of the drug within the formulated hydrogel patch. These findings provide valuable insights into the structural interactions between DCH and the polymer matrix, substantiating the stability and compatibility crucial for an effective drug delivery system.

Determination of absorption maxima

After diluting standard DCH drug solutions with a 7.4 phosphate buffer solution, an analysis was conducted to determine the maximum absorption wavelengths for DCH. Solutions containing 5 mg/ml of each drug were examined across the wavelength range of 200-400 nm. The highest absorbance of DCH was identified at a wavelength of 272 nm.

Weight variation and thickness

The weight variation was determined using a meticulous technique in which three randomly selected patches from each formulation were individually weighed. Patches having an average weight of 2.98 ± 1.89 to 3.63 ± 1.98 g were assessed further using vernier callipers. The thickness measurement was done precisely, with an average value calculated from six estimations collected at the four corners and center of each patch. The patches' average thickness was assessed using a meticulous procedure, resulting in a range of 2.13 ± 2.37 to 2.43 ± 2.63 mm. The consistent thickness of patches in all samples indicates their physical consistency, as shown by the low standard deviation (SD) values. These detailed results underscore the measurement of precision and accuracy in characterizing the physical attributes of the topical hydrogel patches. The resulting thickness range provides valuable insights into the consistency and uniformity of the patches across various formulations and is presented in Table 3.

Table 2: FT-IR analysis Interpretation of drug sample of DCH with polymer

S. No.	Functional group	FT-IR band of doxycycline hyclate (cm^{-1})	FT-IR Band of the drugs sample containing chitosan, HPMC, peg 10000, acrylic acid, carbopol 934, Mba (cm^{-1})
1	O-H stretching	3263.56	3329.14
2	C=O	1660.71	1618.28
3	C-H (Out of plane bending)	935	931.62
4	C-C-C, C-C(=O)-C(Bending)	1215.15	1292.31
5	CO-NH (Amide-II)	1546	1566.40

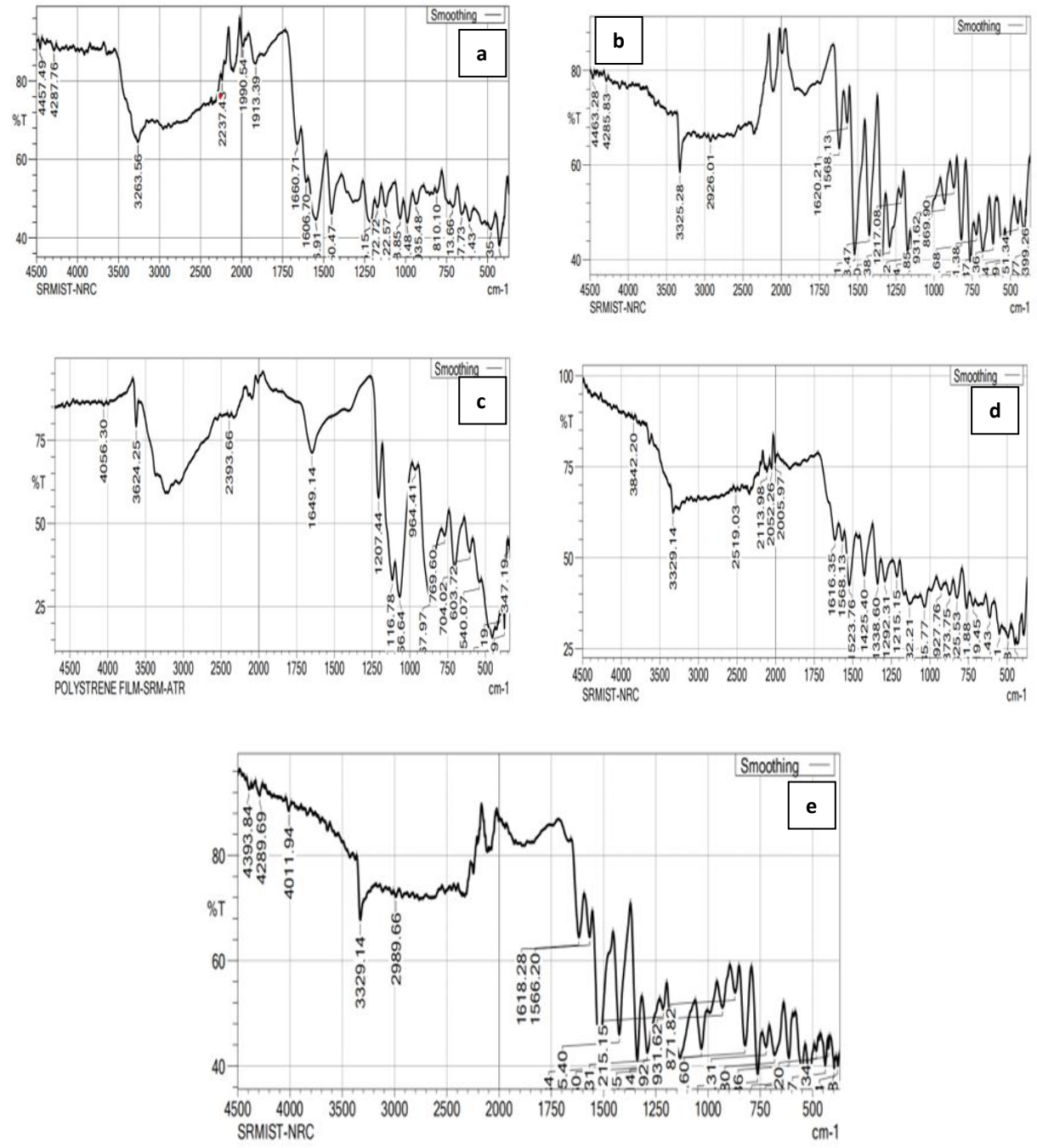

Figure 1: FT-IR spectrum of a) doxycycline hyclate; b) chitosan; c) Peg-10000; d) carbopol 934; and e) selected drug loaded hydrogel patch formulation F6

Folding endurance

The evaluation of the folding endurance of the produced topical hydrogel patches showed positive outcomes, confirming that the patches formed with different amounts of polymers, affirming their flexibility and not being prone to breaking. The folding endurance of formulation F6 was assessed in this study using a manual procedure, which included folding patches up to a maximum of 120 times. During the folding procedure, meticulous attention was devoted to detecting any indications of fragility or fractures in the patches. The findings of each folding experiment were established by meticulously examining the patch for any visible indications of structural damage or fracture. Significantly, the patches produced in the F6 formulation demonstrated durability and maintained their structural integrity over the 120 test folds; no fractures were seen.

The results indicate that the hydrogel patches, especially the formulations with the required concentrations of polymers, have strong mechanical characteristics, demonstrating their suitability for applications that involve frequent folding or bending. The manual evaluation of folding endurance functioned as a reliable method for evaluating the flexibility and durability of the patches, providing valuable insights into their potential use. The folding endurance of the F1 to F7 formulation ranged between 71 ± 0.91 and 84 ± 0.79. Notably, formulation F6 exhibits an enhanced folding endurance of 84 ± 0.79 compared to all other formulations, as indicated in Table 3.

Zeta potential

The results were obtained by selecting an F6 formulated hydrogel patch, as identified by DLS analysis. According to the DLS results, the estimated size of the nanoparticles was 162 nm, and the particle size distribution was 397.3, indicating uniformity in particle size. Moreover, the size determined by the FE-SEM approach and the hydrodynamic diameter determined by the DLS technique are closely aligned. As a result, the CNPs exhibited a zeta potential value of -22.4 mV.

SEM Characterization

The investigation into the surface morphology of the selected formulation F6 hydrogel patch formulation aimed to thoroughly assess its surface texture and characteristics. Utilizing SEM, it has been determined that the hydrogel patch incorporating CNPs exhibited a spherical shape, showcasing a diverse size range spanning from 92.83 nm to 206.2 nm, as depicted in Figure 2. The SEM micrographs further unveiled a distinctive surface profile characterized by a rough and porous structure. This specific porous arrangement plays a vital role in promoting water penetration into the hydrogels, thereby facilitating an enhanced swelling of the formulation. The results derived from this analysis were notably positive, signifying excellent drug entrapment within the formulation matrix. Moreover, the hydrogel patch demonstrated significant promise in practical applications.

Upon exposure to bodily fluids, the formulation exhibited an effective and controlled release of the encapsulated drug. This finding highlights the formulation's potential for therapeutic applications where precise drug delivery and controlled release are crucial aspects of the intended pharmacological impact. Overall, the comprehensive analysis of surface morphology provides valuable insights into the physical attributes and performance capabilities of the hydrogel patch formulation.

X-ray Diffraction (XRD)

XRD analysis was conducted to differentiate the composition of the formulation and the polymer. The crystallinity and amorphous characteristics of the substances were confirmed through XRD analysis of DCH, PEG-10000, and the topical hydrogel patches of the selected formulation F6, as illustrated in Figure 3. The formulation's solubility and release pattern are highly influenced by its crystalline and amorphous properties. The XRD analysis of chitosan and carbopol 934 revealed the absence of significant peaks, showing their amorphous nature.

Table 3: Weight variation, thickness, and folding endurance of formulated patches

Formulation code	Weight variation	Thickness	Folding endurance
F1	2.98 ± 1.89	2.13 ± 2.37	71 ± 0.91
F2	3.19 ± 1.74	2.21 ± 2.84	75 ± 0.89
F3	3.54 ± 1.39	2.17 ± 2.78	80 ± 0.57
F4	3.46 ± 1.69	2.32 ± 2.56	78 ± 0.66
F5	3.63 ± 1.98	2.43 ± 2.63	69 ± 0.74
F6	3.32 ± 1.67	2.19 ± 2.80	84 ± 0.79
F7	3.59 ± 1.54	2.26 ± 2.77	81 ± 0.80

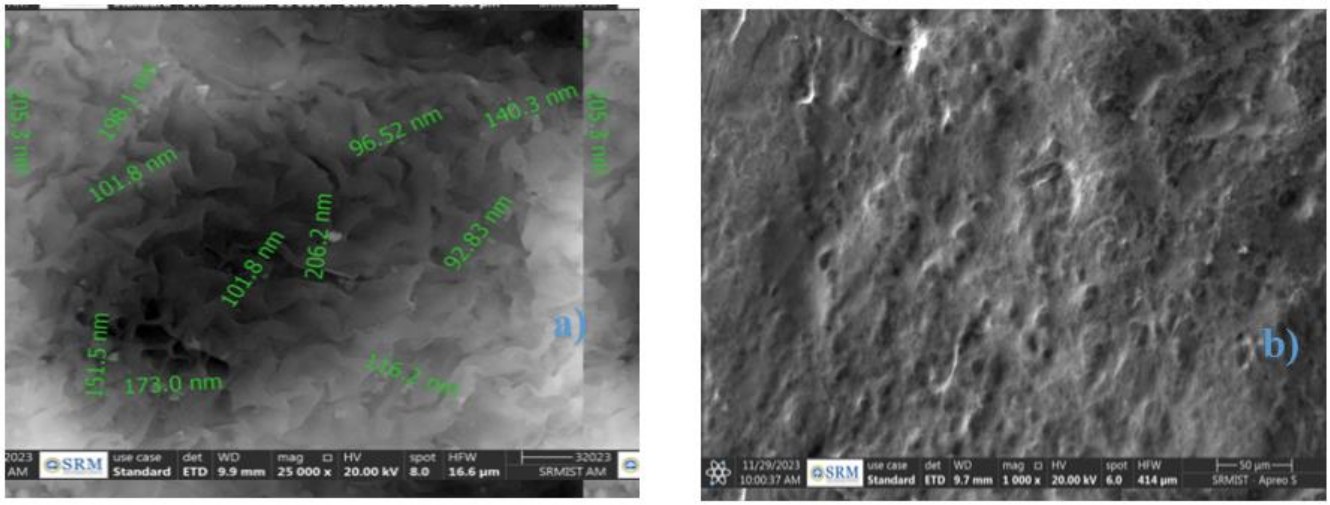

Figure 2: Surface characteristics of the selected formulation observed at varying magnifications a) chitosan nanoparticles loaded with DCH and b) topical hydrogel patch surface structure of an optimized formulation

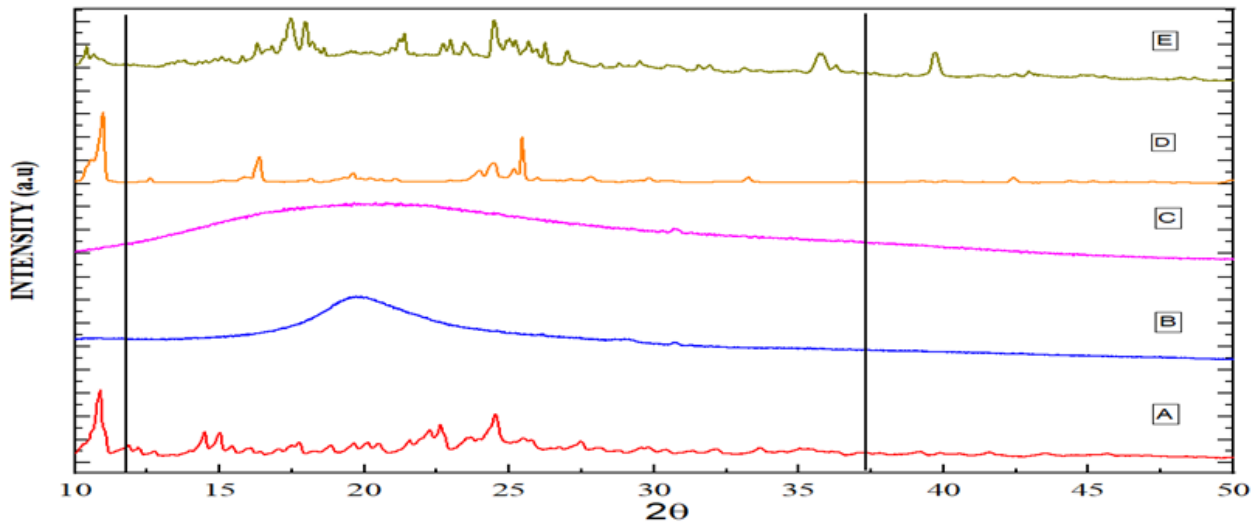

Figure 3: XRD patterns of the A) doxycycline Hyclate, B) chitosan, C) carbopol 934, D) PEG-10000, and E) selected formulation F6 topical hydrogel patch

Differential scanning calorimetry (DSC)

DSC was conducted on the raw polymer and the optimized formulation of the F6 topical hydrogel patch. A DSC 214 polymer was used to study the phase transition properties of deionized water at 10, 20, and 30 K/min charging and discharging rates. Samples weighing 20 to 25 mg were collected in an aluminum crucible with a melting point of 610 °C, while an empty crucible served as a reference. The tests were done in an atmosphere of nitrogen gas at a flow rate of 60 ml/min, and iridium (99.9% pure) was used to

record changes in power and temperature in the DSC measurement. Charging rates were capped at 7 K/min, acknowledging that higher number of specimens intensifies the temperature gradient during rapid charging. Figure 4 illustrates variations in the primary phase transition properties of deionized water, encompassing parameters like enthalpy, peak temperatures, onset temperatures, and end temperatures at different charging and discharging rates. The current DSC analysis focused on a discharge rate of 10 K/min. It is noteworthy that a high flow rate precludes the determination of extract properties. The chosen F6 formulation demonstrated absorption, and during melting, a phase change was observed in DCH. During the freezing process, from 142.7 to 172.6 °C, no change in the phase could be seen. This suggests that the first melting point of the F6 formulation, which is 142.7 °C, broke down. The entire heating process was maintained at 172.6 °C, with the sample exhibiting the maximum heat absorption around 130.7 °C. An additional peak emerged at a revised temperature of 172.6 °C, indicating that the negative area signifies the sample rejecting heat due to environmental factors, with a heat rejection rate measured at 359.4 J/g. Table 4 summarizes the DSC analysis of various materials in the current study.

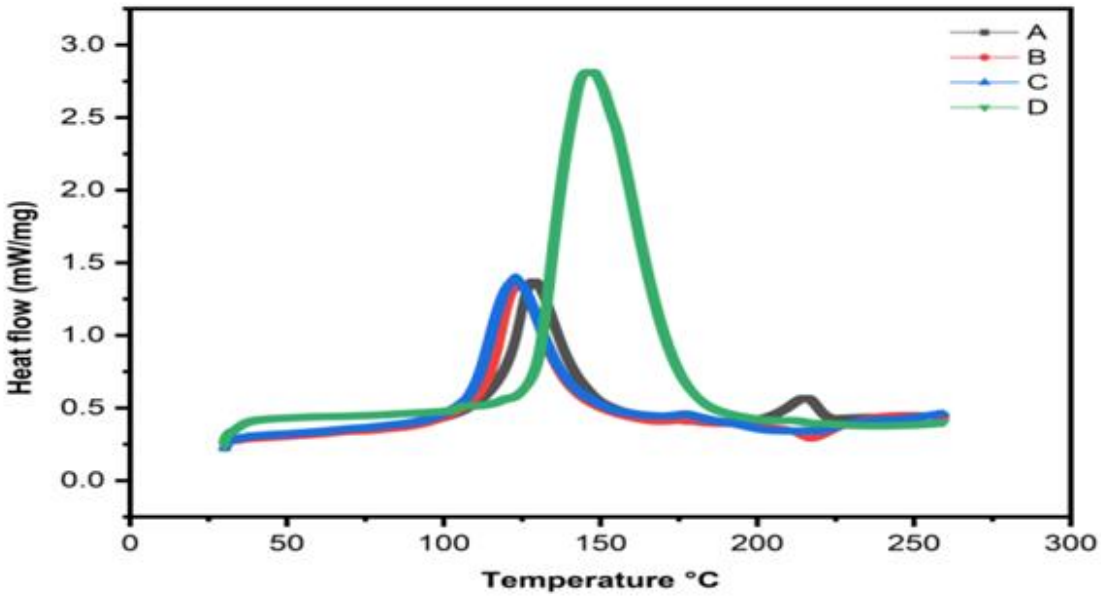

Figure 4: DSC analysis of the A) Doxycycline hyclate, B) PEG-10000, C) physical mixture, and D) selected formulation F6 hydrogel patch

Table 4: Phase change characteristics from DSC analysis

S. No.	Materials	Melting temperature			
		Onset temperature (°C)	End temperature (°C)	Peak temperature (°C)	Fahrenheit temperature J/g
1	Doxycycline hyclate	117.3	146.3	126.4	151.4
2	PEG 10000	114.2	142.7	121.3	137.2
3	Physical mixture	123.7	147.4	129.7	148.5
4	Selected formulation F6 hydrogel patch	130.7	172.6	139.4	359.4

Measurement of pH Value

During the process of developing pH-responsive hydrogels, the pH value is an essential factor that determines both the efficacy and quality of formulations. DCH loaded CNPs cross-linked hydrogel formulations that maintain an appropriate pH range and enhance the development of Schiff base linkages. Typically, the development of linkage formation takes place within the pH range of 4 to 7. The pH values of the blank gel formulations without adding DCH were measured for F1 to F7 as F1-4.22 ± 0.02, F2-5.47 ± 0.04, F3 -5.69 ± 0.02, F4 -5.52 ± 0.02, F5 -5.72 ± 0.02, F6 -5.85 ± 0.02, and F7-5.63 ± 0.02. Consequently, the pH values for the DCH loaded CNPs cross-linked hydrogel formulations, denoted as F1 to F7, were determined to be F1-5.39 ± 0.02, F2-5.98 ± 0.02, F3-6.12 ± 0.02, F4-6.86 ± 0.02, F5-7.14 ± 0.02, F6-7.47 ± 0.02, and F7-7.23 ± 0.02, confirming their suitability for Schiff base bond formation while formulation F6 was found to have the highest pH value, ranging from 5.39 ± 0.02 to 7.47 ± 0.02. Moreover, the results revealed a significant difference between blank gel and blank gel loaded with DCH within the same formula ($p < 0.05$). Also, F1, the mixture that had DCH added, was less stable. This might be because carbopol 934 breaks down easily at pH levels lower than 4.5. This observed variation may potentially not affect the release rate of the drug at the F1 formulation onto the wound skin surface of diabetic foot ulcers (DFU), characterized by a pH range of 5.4-8.9. This variation underscores the importance of pH control in the formulation, addressing both the stability and potential therapeutic effectiveness of the hydrogel system.

Rheology studies

The mechanical attributes were investigated, such as viscosity, rheology, and gel strength, to assess the material's efficiency. The findings revealed that increased concentrations of carbopol 934 and HPMC resulted in higher gel viscosity. In addition, the viscosity of hydrogels was impacted by the pH of each formulation, with hydrogels containing Schiff base linkages exhibiting a reduction in viscosity at lower pH values. The strength of the cross-links had a substantial effect on the connectivity of the pores inside the gel. The addition of DCH, polymers, cross-linkers, and monomers to the system aided in its development, resulting in an obvious increase in the gel's viscosity. This phenomenon indicates that drug incorporation helps to contribute stronger cross-links within the gel matrix, changing pore connectivity and possibly affecting the gel's overall performance and characteristics. In this study, viscosity (cP) formulations range between F1 and F7, as presented in Table 5. Each formulation demonstrated pseudo-plastic characteristics. The rheological investigations were conducted on the hydrogel at different shear rates. The findings demonstrated a reciprocal correlation between shear rate and hydrogel viscosity, indicating that as shear rate increased, hydrogel viscosity decreased, and vice versa.

This characteristic enhances and improves comfort and usability, increasing the accessibility of the formulations. In addition, gel strength tests were conducted to evaluate the resilience of hydrogel, so it is an important aspect in providing the integrity of gel formulations for optimum drug release at the specific target area. The gel-strength formulations varied from F1 to F7, as shown in Table 5. Gel strength studies were performed to confirm the flexibility of DCH loaded CNPs cross-linked in the hydrogel, which is essential for maintaining the integrity of the gel formulations to provide effective drug release at the specified target site. Gel strength was determined based on the G'/G'' value. This observation aligns with the results of the viscosity study, suggesting that an increase in gel strength is correlated with an increase in viscosity. Formulation F6 is highly suitable for applications in DFU healing.

Hydrogel swelling characteristics: Influence of polymer, monomer, and cross-linker

Table 5: Viscosity and gel strength of prepared formulations

Formulation code	Viscosity (cP)	Gel strength (g/cm^2)
F1	1100	527
F2	1316	538
F3	1392	559
F4	1490	583
F5	1456	569
F6	1547	591
F7	1488	578

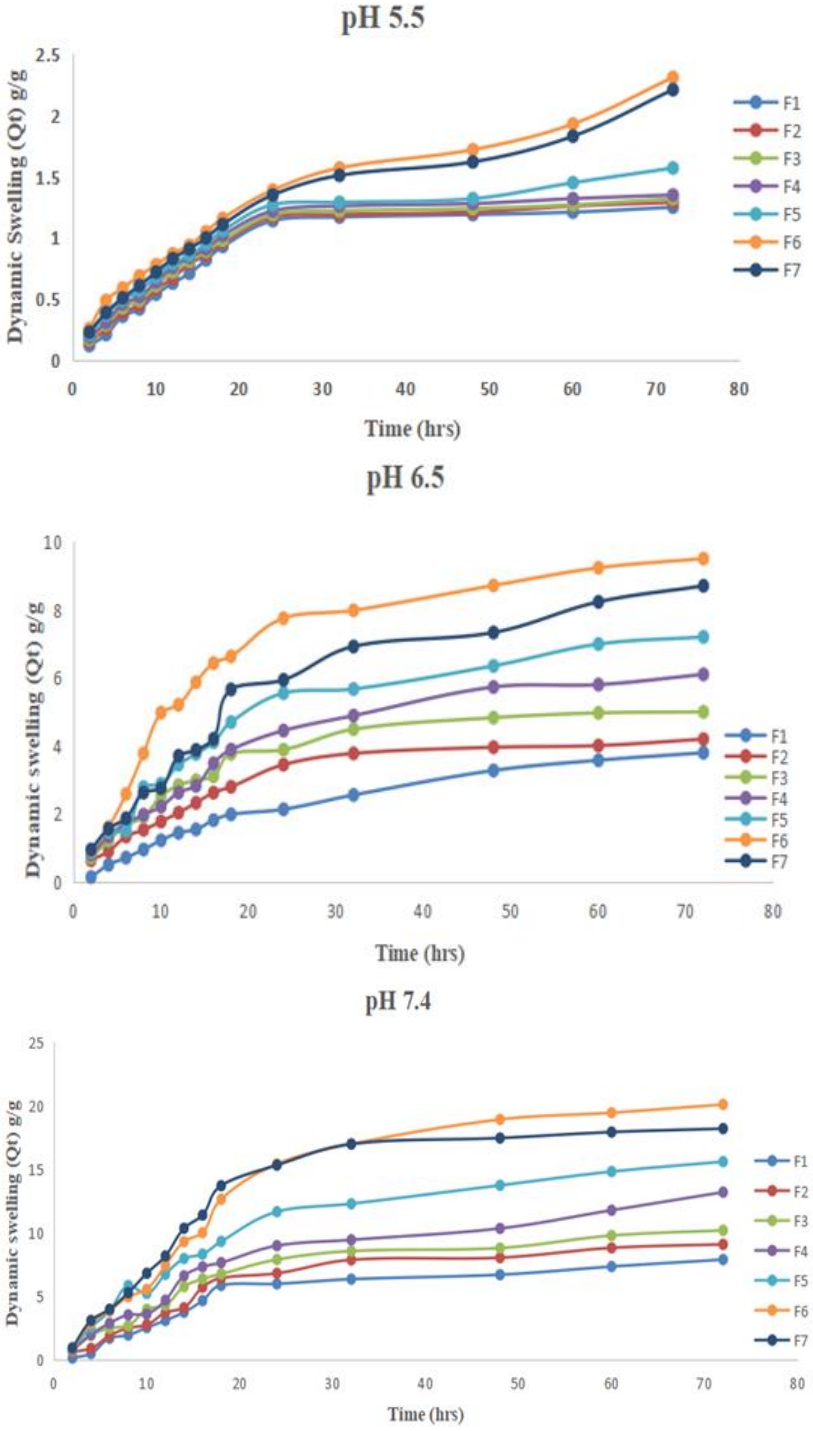

Figure 5: Swelling dynamics release graph of formulations F1 to F7 at various pH levels a) 5.5; b) 6.5; and c) pH 7.4

The chitosan nanoparticle cross-linked hydrogel patches were meticulously formulated, incorporating different concentrations of polymers like PEG-10000, HPMC, acrylic acid, and methylene bisacrylamide. An analysis of the polymeric networks' behavior in swelling was done in buffer solutions. The impact of the polymeric networks' hydrophilicity on swelling and drug release is significant. The swelling behavior was observed until a stable weight was achieved. Due to its elevated concentrations of OH and COOH groups, PEG-10000 is pH-sensitive and therefore particularly desirable in alkaline environments. Formulations F1 to F7, featuring increasing polymer concentrations, exhibited increasing swelling. Water inhibition was enhanced as a result of the ionization and electrostatic repulsion of functional groups induced by the greater quantity of PEG-10000 molecules. All formulated hydrogel patches demonstrated increased swelling, especially at pH 7.4. This was due to the polymeric chain being ionized, which greatly improved its ability to absorb water. The series of formulations F1, F2, F3, F4, and F6 with increasing concentrations of acrylic acid demonstrated heightened swelling, particularly in F6. At higher pH levels, the hydrogel polymeric networks observed an increase in swelling due to the higher concentration of acrylic acid, which resulted in the formation of more carboxylic groups. As a result of the ionization of carboxylic groups, a higher concentration of negatively charged COO^- groups was produced, resulting in a surge in osmotic pressure and electrostatic repulsion. Subsequently, this promoted additional swelling expansion and enlargement of the network of cross-linked polymers.

In contrast, series F5 and F7 with increasing concentrations of methylene bisacrylamide exhibited reduced swelling. The size reduction can be attributed to a denser structure that limits the gaps between polymeric networks, thus restricting the relaxation and expansion of hydrogel chains and hydrogel swelling. The optimized formulation revealed the temporal progression of swelling at different pH levels, providing valuable insights into swelling in response to varying pH conditions illustrated in Figure 5.

Spreadability

The spreadability evaluation was conducted for both the blank hydrogel and the hydrogel loaded with nanoparticles. The results indicate a spreadability value of 364.75 ± 0.39 mm^2 for the blank hydrogel and 263.7 ± 0.47 mm^2 for the DCH loaded CNPs cross-linked hydrogel. The observed spreadability ranges within this specified range affect the ease with which the gel can be applied and spread smoothly on the skin surface. This range ensures optimal and comfortable spreading properties for the hydrogel.

Sol-gel analysis

In the series of formulations from F1 to F7, sol-gel analyses revealed varying gel fractions: F1-91.2%, F2-93.3%, F3-94.8%, F4-96.4%, F5-97.2%, F6-99.1%, and F7-98.7%. The gel fraction showed enhancement with an increase in polymer quantity, reaching its maximum peak at 99.1% in the F6 formulation. In the F4 formulation, the polymer concentration remained constant while the monomer concentration (AA) was increased. The results of the study showed that there was a progressive rise in the gel fraction that occurred in combination with an increase in the concentration of the monomer.

An increase in the concentrations of both the monomer and polymer results in greater availability of functional groups and active sites accessible for free radical polymerization. Thus, there is an increase in bioavailability. This leads to a higher gel fraction and is responsible for the formation of a hydrogel that is more stable. The gel fraction of formulations F6 and F7 increased significantly due to the elevated concentration of MBA, which rose from 99.1% to 98.7%. A sol fraction study was performed to measure the unreacted reactants (polymer, cross-linker, and monomer) used in the fabrication of CNP hydrogel patches. The results confirmed the effective development of CNPs cross-linked topical hydrogel patches by revealing a minimal fraction of sol-gel analysis.

Table 6: Drug entrapment efficiency

Formulation code	% of drug loading	% of Drug entrapment efficiency
F1	89	77
F2	86	73
F3	87	75
F4	83	71
F5	90	76
F6	92	79
F7	85	74

Table 7: *In vitro* drug release studies of DCH loaded CNPs cross-linked hydrogel patches

Formulation code	Time (h)	% drug release (%± SD)		
		pH 5.5	pH 6.5	pH 7.4
F1	72	52.52 ± 0.532	56.46 ± 0.512	91.46 ± 0.562
F2	72	57.65 ± 0.423	58.71 ± 0.472	93.71 ± 0.463
F3	72	59.24 ± 0.475	61.53 ± 0.415	94.53 ± 0.415
F4	72	62.52 ± 0.534	64.97 ± 0.464	94.97 ± 0.514
F5	72	63.92 ± 0.386	66.43 ± 0.392	95.43 ± 0.426
F6	72	65.26 ± 0.534	71.21 ± 0.531	97.21 ± 0.524
F7	72	64.17 ± 0.427	68.18 ± 0.419	96.18 ± 0.433

Impact of materials on gel%, yield%, and gel time in hydrogel patch formulation

In the series of hydrogel patch formulations, which range from F1 to F7, a distinct pattern appeared, demonstrating an increase in gel percentage and yield percentage, as well as a concurrent reduction in gel duration as the polymer concentration of PEG-10000 increased. This trend was reflected in the formulation series from F4 to F6, where increasing the monomer content resulted in a greater gel percentage and yield percentage while decreasing the gelling time. This observed tendency is attributed to the heightened active sites available for free radical polymerization, used by higher polymer and monomer concentrations. This phenomenon accelerates the early tangling of polymeric chains, facilitating the gelation process. Furthermore, an increase in MBA concentration led to a reduction in gel time and an increased gel percentage and yield percentage. The presence of the cross-linker acted as a catalyst, enhancing the reaction rate and expediting the rapid formation of polymeric chains. This increased the gel% and yield% values. The parameters include yield%, gel%, and gel time for PEG-10000, monomer, and cross-linker, respectively, and were carefully monitored. The increased gel% and yield% values collectively signify the successful development of the formulations, with all formulations demonstrating over 85% gel and yield percentages. Significantly, the gelling time, a crucial aspect in the formulation process, experienced a consistent reduction, aligning with the overall trend of enhanced gelation efficiency with varying concentrations of monomer, polymer, and cross-linker. Based on these results, it can be stated that the formulation of the polymeric cross-linked hydrogel patch was quite effective.

Drug content and drug entrapment efficiency (%)

The evaluation of the drug entrapment efficiency was conducted on the developed formulation series ranging from F1 to F7. It was found that the formulation with the highest polymer concentration exhibited notable results in terms of drug entrapment efficiency; the results are presented in Table 6.

In vitro drug release study

In vitro drug release studies were carried out on DCH loaded CNPs cross-linked in hydrogel patches to evaluate their release behavior in phosphate buffer at varying pH levels of 5.5, 6.5, and 7.4. At pH 7.4, a release exceeding 97.21 ± 0.524% was observed. When compared to pH levels of 5.5 and 6.5. The *in vitro* drug release from the prepared patch formulations at pH 7.4 showed the following findings: F1-DCH-91.46 ± 0.562%, F2-DCH-93.71 ± 0.463%, F3-DCH-94.53 ± 0.415%, F4-DCH-94.97 ± 0.514%, F5-DCH-95.43 ± 0.426%, F6-DCH-97.21 ± 0.524%, and F7-96.18 ± 0.433%. Formulation F6 exhibited the highest percentage of drug release with DCH at 72 h of about 97.21 ± 0.524% illustrated in Figure 6. When the pH level was elevated, there was less hydrogen bonding occurring between the OH groups of PEG-10000 and more electrostatic repulsion. This resulted in an expansion of the polymeric network mesh size, allowing a greater influx and efflux of water molecules inside the formulation, hence explaining the observed enhancement in drug release.

Formulations F4 to F6 exhibited escalating drug release with an incremental monomer concentration. F6 demonstrated the highest drug release over 72 hours due to its pH value. In formulations F1 through F5, the drug release is reduced, which may be attributed to the increased amounts of cross-linker. The F7 formulation had a larger proportion of cross-linkers, which resulted in much stronger hydrogen bonding. The decrease in electrostatic repulsion resulted in a more compact polymeric structure, limiting drug release. The drug release percentages of the optimized formulation F6 are specified in Table 7. This comprehensive analysis highlights the complex interaction among the constituents of the formulation, impacting the dynamics of drug release from hydrogel patches with DCH in a polymeric cross linked matrix.

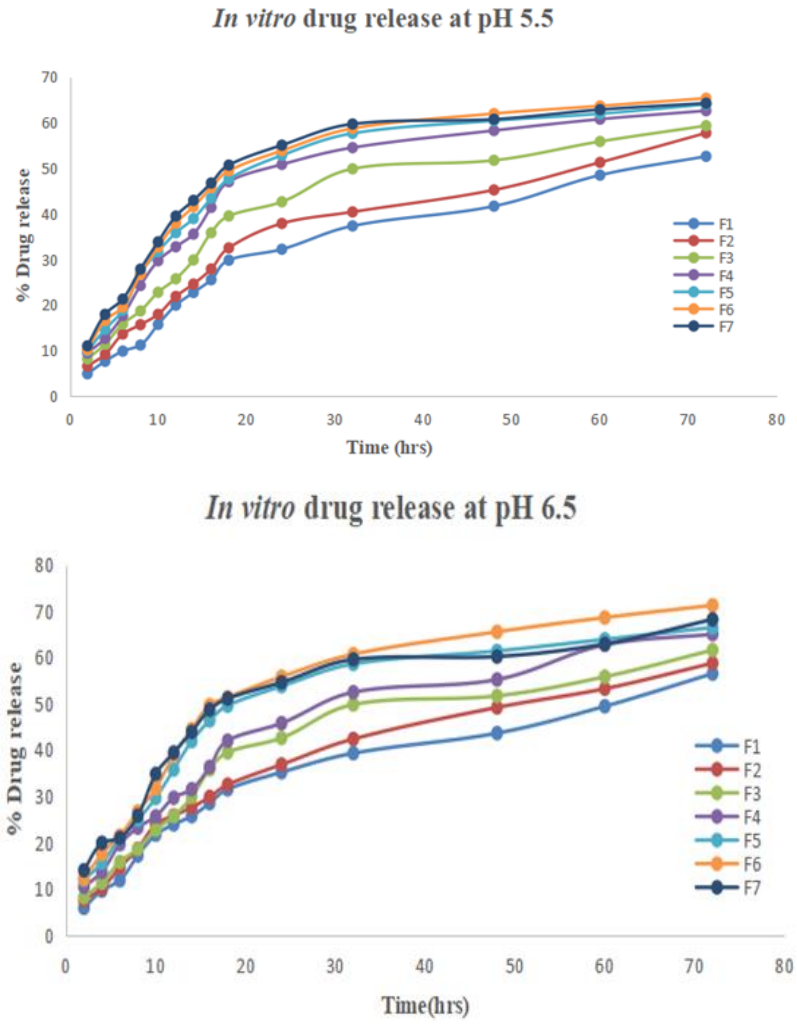

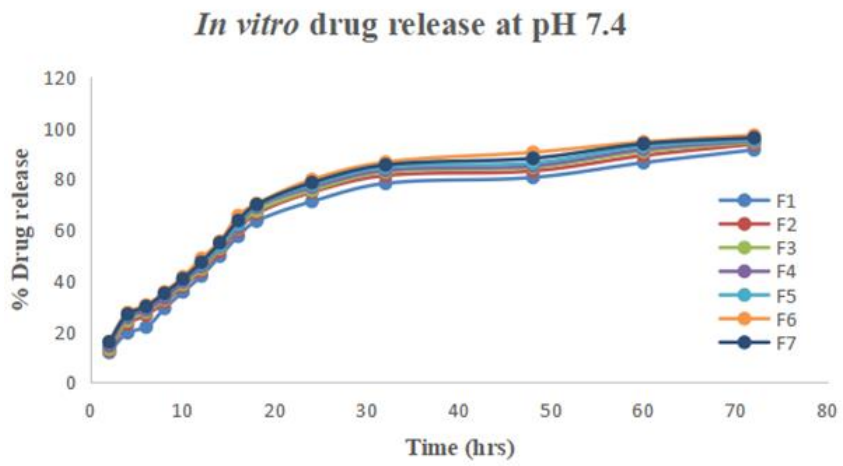

Figure 6: % *In vitro* drug release of formulations F1 and F7 at different pH levels

Table 8: *In vitro* kinetic modeling drug release analysis for all formulations

Formulation code	Zero-order R^2	First order R^2	Hixon Crowell R^2	Higuchi model R^2	Korsmeyer Peppas R^2	*n* value
F1	0.9953	0.9922	0.9942	0.9742	0.9782	0.527
F2	0.9937	0.9933	0.9934	0.9756	0.9756	0.532
F3	0.9946	0.9892	0.9933	0.9624	0.9689	0.512
F4	0.9935	0.9924	0.9947	0.9667	0.9721	0.546
F5	0.9941	0.9937	0.9939	0.9715	0.9774	0.581
F6	0.9975	0.9961	0.9953	0.9792	0.9798	0.572
F7	0.9957	0.9949	0.9946	0.9649	0.9757	0.564

In vitro drug deposition study using a semipermeable synthetic membrane

Hydrogel formulation F6, selected for drug deposition studies, showed promising results in terms of drug permeation through a semipermeable synthetic membrane with an area of 1.5 cm^2.

The investigation focused on the permeability of the drug DCH, and the observations displayed that the amount of drug permeated was notably higher at pH 7.4 than at 6.5 and 5.5. The research focused on measuring the permeability flux (Jss) and permeability coefficient (Kp), which were important parameters to measure during the study. The DCH loaded hydrogel patch exhibited permeability fluxes of pH 5.5-0.8274, pH 6.5-1.2135, and 1.46842 µg/cm^2/h at a pH of 7.4. The permeability coefficient (Kp) ranges were found at pH 5.5–1.514 × 10^{-6}, pH 6.5-2.314 × 10^{-6}, and pH 7.4-2.814 × 10^{-6} cm/h. These indicate the efficacy of the hydrogel formulation in promoting drug absorption across the synthetic membrane.

The application of kinetic analysis to the permeation data showed a consistent drug release pattern from the patch; a zero-order pattern was followed over time. The drug penetration from the hydrogel patch was determined to be diffusion-controlled, as shown by the kinetic study. This finding implies that the drug molecules diffused through the semipermeable synthetic membrane in a regulated manner, enhancing the predictability and control of drug release. Importantly, the results consistently demonstrated that drug permeation was significantly higher at pH 7.4. The hydrogel formulation is optimized for drug release at a slightly basic pH, enhancing drug permeation at pH 7.4, allowing the drug to remain on infected skin surface, potentially improving the effectiveness of patches. The hydrogel formulation is optimized for drug release at a slightly basic pH, enhancing drug permeation at pH 7.4, allowing the drug to

remain on infected skin surface, potentially improving the effectiveness of patches.

In conclusion, the drug's *in vitro* availability through the hydrogel formulation F6 across the skin was seen to be much better. The formulation showed a controlled and sustained drug release profile. Further highlights the potential applicability of this hydrogel in targeted drug delivery for localized treatment in DFU healing.

Drug release kinetic modeling study

The evaluation study was conducted on the drug release kinetics of DCH loaded CNPs cross-linked topical hydrogel patches and was analyzed using a systematic evaluation of various kinetic models, such as zero-order, first-order, Hixon Crowell, Higuchi, and Korsmeyer peppas models, as provided in Table 8. The drug release data results were obtained using stimulation plus software, which played an essential role in determining the release pattern of the intended drug delivery system. A consistent drug release pattern was observed in all seven formulations, as evidenced by regression coefficients R^2 ranging from 0.9935 to 0.9975, which all adhered to zero-order kinetics. The applicability of the Higuchi model was confirmed, with regression coefficients R^2 showing a range of 0.9624 to 0.9792. According to these results, the drug concentration of the substance did not affect the drug release from the hydrogel matrix in the patch. This indicates the presence of a process that is based on a diffusion mechanism, which is probably connected to the formation of pores within the polymeric matrix. The developed formulations had a nice porous structure that prevented water from passing through it and allowed the drug to diffuse freely from the matrix.

In addition, the value of the "n" exponent ranges from 0.512 to 0.581. Furthermore, the kinetic release study adds to the evidence for the diffusion-controlled release mechanism and shows how reliable the formulation-controlled drug release profile is. The data shows that the drug loaded CNPs cross-linked in topical hydrogel patches are effective at controlling the release of drugs in a detailed and effective way.

Stability studies

The stability analysis of the formulated hydrogel patch was meticulously conducted, adhering to the guidelines outlined by the ICH, under a range of different temperature conditions. The selected F6 hydrogel patch formulation underwent rigorous stability testing, revealing insightful results. As summarized in Tables 9, 10, 11, and 12, these results indicated slight modifications or degradation, which appeared to be contingent on the concentration or quantity of the drug components in the formulations.

Table 9: Stability analysis for selected formulation F6 at 25±0.5 °C and 60±5% R

S. No.	RH/Conditions	Time intervals	% Drug release DCH	Phase separation	Appearance	Grittiness
1	25±0.5 °C & 60±5% RH	Initial	96.26 ± 0.544	No	Transparent dry non-sticky flexible	None
2		1	96.13 ± 0.512	No		None
3		2	95.92 ± 0.492	No		None
4		3	95.62 ± 0.495	No		None
5		6	95.24 ± 0.487	No		None

Table 10: Stability analysis for selected formulation F6 at 30±0.5 °C and 65±5% RH

S. No.	RH/Conditions	Time intervals	% Drug release DCH	Phase separation	Appearance	Grittiness
1	30±0.5 °C & 65±5% RH	Initial	96.26 ± 0.544	No	Transparent dry non-sticky flexible	None
2		1	95.92 ± 0.524	No		None
3		2	95.75 ± 0.492	No		None
4		3	94.93 ± 0.481	No		None
5		6	94.53 ± 0.471	No		None

Table 11: Stability analysis for selected formulation (F6) at 30±0.5 °C and 75±5% RH

S.no	RH/Conditions	Time intervals	% Drug release DCH	Phase separation	appearance	Grittiness
1	30±0.5 °C & 65±5% RH	Initial	96.26 ± 0.544	no	Transparent dry non-sticky flexible	none
2		1	95.85 ± 0.522	no		none
3		2	95.61 ± 0.483	no		none
4		3	94.52 ± 0.472	no		none
5		6	94.11 ± 0.468	no		none

Table 12: Stability analysis for selected formulation F6 at 40±0.5 °C and 75±5% RH

S.No.	RH/Conditions	Time intervals	% Drug release DCH	Phase separation	Appearance	Grittiness
1	40±0.5 °C and 75±5% RH	Initial	96.26 ± 0.544	No	Transparent dry non-sticky flexible	None
2		1	95.72 ± 0.519	No		None
3		2	95.49 ± 0.477	No		None
4		3	94.56 ± 0.471	No		None
5		6	93.47 ± 0.463	No		None

This comprehensive analysis shows valuable insights into the formulation's long-term stability and its potential to maintain quality and effectiveness under various storage conditions [40].

Conclusion

The study demonstrates that DCH loaded CNPs cross-linked topical hydrogel patches are effective in free radical polymerization. The hydrogel patches were evaluated for appearance, morphology, crystallinity, thermodynamic stability, swelling behavior, and drug release patterns. The drug penetration across the skin was assessed, and *in vitro* release studies were conducted using a semi-synthetic membrane. The efficacy and sensitivity of the therapy were assessed.

The formulation with the highest concentrations of polymer and monomer and the lowest concentration of cross-linker showed the most significant swelling and the highest percentage of drug release. The formulation also demonstrated enhanced drug permeation into the skin, maintaining a steady release profile. All formulations exhibited sensitivity to changes in pH. Formulation F6 emerged as the most suitable option. The evaluation process involved various techniques, including XRD, Zeta potential, SEM, DSC, and various physicochemical parameters. *In vitro* drug release studies were conducted with Franz diffusion cells, and stability studies were performed over six months. The results indicate that the DCH loaded CNPs cross-linked topical hydrogel patches are highly suitable for controlled drug release on the surface of wounded skin, providing both local and systemic advantages for diabetic foot ulcers (DFU) and controlling DFU infections. Further *in vivo* studies are planned to examine the pharmacokinetic profile characteristics of these patches.

Disclosure Statement

No potential conflict of interest was reported by the authors.

Funding

This research did not receive any specific grant from funding agencies in the public, commercial, or not-for-profit sectors.

Authors' Contributions

All authors contributed to data analysis, drafting, and revising of the paper and agreed to be responsible for all the aspects of this work.

Abbreviations

DFU - Diabetic foot ulcer

DCH - Doxycycline hyclate
CNPs - Chitosan nanoparticles
PEG - Polyethylene Glycol
DMSO - Dimethyl sulfoxide
Aps - Ammonium persulfate
AA - Acrylic Acid
MBA - Methylenebisacrylamide
STPP - Sodium tripolyphosphate
FT-IR - Fourier transform infrared spectroscopy
DSC - Differential Scanning Calorimetry
XRD - X-ray diffraction analysis
SEM - Scanning electron microscopy

ORCID

Sidhavatam Harshavardhan Reddy
https://orcid.org/0000-0003-1556-5912
Manimaran V
https://orcid.org/0000-0003-2404-6268

References

[1]. Güiza-Argüello V.R., Solarte-David V.A., Pinzón-Mora A.V., Ávila-Quiroga J.E., Becerra-Bayona S.M., Current advances in the development of hydrogel-based wound dressings for diabetic foot ulcer treatment, *Polymers*, 2022, **14**:2764 [Crossref], [Google Scholar], [Publisher]
[2]. Hu B., Gao M., Boakye-Yiadom K.O., Ho W., Yu W., Xu X., Zhang X.Q., An intrinsically bioactive hydrogel with on-demand drug release behaviors for diabetic wound healing, *Bioactive Materials*, 2021, **6**:4592 [Crossref], [Google Scholar], [Publisher]
[3]. Jodheea-Jutton A., Hindocha S., Bhaw-Luximon A., Health economics of diabetic foot ulcer and recent trends to accelerate treatment, *The Foot*, 2022, **52**:101909 [Crossref], [Google Scholar], [Publisher]
[4]. Hicks C.W., Canner J.K., Mathioudakis N., Lippincott C., Sherman R.L., Abularrage C.J., Incidence and risk factors associated with ulcer recurrence among patients with diabetic foot ulcers treated in a multidisciplinary setting, *Journal of Surgical Research*, 2020, **246**:243 [Crossref], [Google Scholar], [Publisher]
[5]. Cui S., Sun X., Li K., Gou D., Zhou Y., Hu J., Liu Y., Polylactide nanofibers delivering doxycycline for chronic wound treatment, *Materials Science and Engineering: C*, 2019, **104**:109745 [Crossref], [Google Scholar], [Publisher]
[6]. Laturkar K., Bompilwar E., Polshettiwar S., Jagdale S., Kuchekar B., Overview on doxycycline- and its adverse reactions, *International Journal of Advances in Pharmacy and Biotechnology*, 2021, **7**:8 [Crossref], [Google Scholar], [Publisher]
[7]. Chang M., Nguyen T.T., Strategy for treatment of infected diabetic foot ulcers, *Accounts of Chemical Research*, 2021, **54**:1080 [Crossref], [Google Scholar], [Publisher]
[8]. Bai H., Kyu-Cheol N., Wang Z., Cui Y., Liu H., Liu H., Feng Y., Zhao Y., Lin Q., Li Z., Regulation of inflammatory microenvironment using a self-healing hydrogel loaded with BM-MSCs for advanced wound healing in rat diabetic foot ulcers, *Journal of Tissue Engineering*, 2020, **11**:2041731420947242 [Crossref], [Google Scholar], [Publisher]
[9]. Ahmad Z., Khan M.I., Siddique M.I., Sarwar H.S., Shahnaz G., Hussain S.Z., Bukhari N.I., Hussain I., Sohail M.F., Fabrication and characterization of thiolated chitosan microneedle patch for transdermal delivery of tacrolimus, *AAPS PharmSciTech*, 2020, **21**:1 [Crossref], [Google Scholar], [Publisher]
[10]. Laturkar K., Bompilwar E., Polshettiwar S., Jagdale S., Kuchekar B., Overview on doxycycline- and its adverse reactions, *International Journal of Advances in Pharmacy and Biotechnology*, 2021, **7**:8 [Crossref], [Google Scholar], [Publisher]
[11]. Hu C., Long L., Cao J., Zhang S., Wang Y., Dual-crosslinked mussel-inspired smart hydrogels with enhanced antibacterial and angiogenic properties for chronic infected diabetic wound treatment via pH-responsive quick cargo release, *Chemical Engineering Journal*, 2021, **411**:128564 [Crossref], [Google Scholar], [Publisher]
[12]. Mo F., Jiang K., Zhao D., Wang Y., Song, J., Tan W., DNA hydrogel-based gene editing and drug delivery systems, *Advanced Drug Delivery Reviews*, 2021, **168**:79 [Crossref], [Google Scholar], [Publisher]
[13]. Bordbar-Khiabani A., Gasik M., Smart hydrogels for advanced drug delivery systems, *International Journal of Molecular Sciences*, 2022, **23**:3665 [Crossref], [Google Scholar], [Publisher]

[14]. Tallapaneni V., Mude L., Pamu D., Palanimuthu V.R., Magham S.V., Karri V.V.S.R., Parvathaneni M., Growth factor loaded thermo-responsive injectable hydrogel for enhancing diabetic wound healing, *Gels*, 2022, **9**:27 [Crossref], [Google Scholar], [Publisher]
[15]. Hedayatyanfard K., Khoulenjani S.B., Abdollahifar M.A., Amani D., Habibi B., Zare F., Asadirad A., Pouriran R., Ziai S.A., Chitosan/PVA/Doxycycline film and nanofiber accelerate diabetic wound healing in a rat model, *Iranian Journal of Pharmaceutical Research: IJPR*, 2020, **19**:225 [Crossref], [Google Scholar], [Publisher]
[16]. Kesharwani P., Bisht A., Alexander A., Dave V., Sharma S., Biomedical applications of hydrogels in drug delivery system: An update, *Journal of Drug Delivery Science and Technology*, 2021, **66**:102914 [Crossref], [Google Scholar], [Publisher]
[17]. Khalid A., Sarwar H.S., Sarfraz M., Sohail M.F., Jalil A., Jardan Y.A.B., Arshad R., Tahir I., Ahmad Z., Formulation and characterization of thiolated chitosan/polyvinyl acetate based microneedle patch for transdermal delivery of dydrogesterone, *Saudi Pharmaceutical Journal*, 2023, **31**:669 [Crossref], [Google Scholar], [Publisher]
[18]. Singh Malik D., Mital N., Kaur G., Topical drug delivery systems: a patent review, *Expert Opinion on Therapeutic Patents*, 2016, **26**:213 [Crossref], [Google Scholar], [Publisher]
[19]. Alshimaysawee S., Fadhel Obaid R., Al-Gazally M.E., Alexis Ramírez-Coronel A., Bathaei M.S., Recent advancements in metallic drug-eluting implants, *Pharmaceutics*, 2023, **15**:223 [Crossref], [Google Scholar], [Publisher]
[20]. Hasan N., Cao J., Lee J., Kim H., Yoo J.W., Development of clindamycin-loaded alginate/pectin/hyaluronic acid composite hydrogel film for the treatment of MRSA-infected wounds, *Journal of Pharmaceutical Investigation*, 2021, **51**:597 [Crossref], [Google Scholar], [Publisher]
[21]. Xiao S., Zhao Y., Jin S., He Z., Duan G., Gu H., Xu H., Cao X., Ma C., Wu J., Regenerable bacterial killing–releasing ultrathin smart hydrogel surfaces modified with zwitterionic polymer brushes, *E-Polymers*, 2022, **22**:719 [Crossref], [Google Scholar], [Publisher]
[22]. Wang S., Chi J., Jiang Z., Hu H., Yang C., Liu W., Han B., A self-healing and injectable hydrogel based on water-soluble chitosan and hyaluronic acid for vitreous substitute, *Carbohydrate Polymers*, 2021, **256**:117519 [Crossref], [Google Scholar], [Publisher]
[23]. Carrillo-Castillo T.D., Luna-Velasco A., Zaragoza-Contreras E.A., Castro-Carmona J.S., Thermosensitive hydrogel for in situ-controlled methotrexate delivery, *E-Polymers*, 2021, **21**:910 [Crossref], [Google Scholar], [Publisher]
[24]. Narayanaswamy R., Torchilin V.P., Hydrogels and their applications in targeted drug delivery, *The Road from Nanomedicine to Precision Medicine*, 2020, 1117 [Google Scholar], [Publisher]
[25]. Amin M.C.I.M., Ahmad N., Halib N., Ahmad I., Synthesis and characterization of thermo-and pH-responsive bacterial cellulose/acrylic acid hydrogels for drug delivery, *Carbohydrate Polymers*, 2012, **88**:465 [Crossref], [Google Scholar], [Publisher]
[26]. Kamoun E.A., Kenawy E.R.S., Chen X., A review on polymeric hydrogel membranes for wound dressing applications: PVA-based hydrogel dressings, *Journal of Advanced Research*, 2017, **8**:217 [Crossref], [Google Scholar], [Publisher]
[27]. Le A.N.M., Nguyen T.T., Ly K.L., Dai Luong T., Ho M.H., Tran N.M.P., Dang N.N.T., Van Vo T., Tran Q.N., Nguyen T.H., Modulating biodegradation and biocompatibility of in situ crosslinked hydrogel by the integration of alginate into N, O-carboxylmethyl chitosan–aldehyde hyaluronic acid network, *Polymer Degradation and Stability*, 2020, **180**:109270 [Crossref], [Google Scholar], [Publisher]
[28]. Xia L., Wang S., Jiang Z., Chi J., Yu S., Li H., Zhang Y., Li L., Zhou C., Liu W., Hemostatic performance of chitosan-based hydrogel and its study on biodistribution and biodegradability in rats, *Carbohydrate Polymers*, 2021, **264**:117965 [Crossref], [Google Scholar], [Publisher]
[29]. Lin C.C., Anseth K.S., PEG hydrogels for the controlled release of biomolecules in regenerative medicine, *Pharmaceutical Research*,

2009, **26**:631 [Crossref], [Google Scholar], [Publisher]
[30]. Reddy B.V., Rao G.R., Vibrational spectra and modified valence force field for N, N′-methylenebisacrylamide, *Indian Journal of Pure and Applied Physics*, 2008, **49**:611 [Google Scholar], [Publisher]
[31]. Jayaramudu T., Raghavendra G.M., Varaprasad K., Reddy G.V.S., Reddy A.B., Sudhakar K., Sadiku E.R., Preparation and characterization of poly (ethylene glycol) stabilized nano silver particles by a mechanochemical assisted ball mill process, *Journal of Applied Polymer Science*, 2016, **133**:43027 [Crossref], [Google Scholar], [Publisher]
[32]. Ranjha N.M., Ayub G., Naseem S., Ansari M.T., Preparation and characterization of hybrid pH-sensitive hydrogels of chitosan-co-acrylic acid for controlled release of verapamil, *Journal of Materials Science: Materials in Medicine*, 2010, **21**:2805 [Crossref], [Google Scholar], [Publisher]
[33]. Alsarra I.A., Chitosan topical gel formulation in the management of burn wounds, *International Journal of Biological Macromolecules*, 2009, **45**:16 [Crossref], [Google Scholar], [Publisher]
[34]. Khan S., Batchelor H., Hanson P., Saleem I.Y., Perrie Y., Mohammed A.R., Dissolution rate enhancement, in vitro evaluation and investigation of drug release kinetics of chloramphenicol and sulphamethoxazole solid dispersions, *Drug Development and Industrial Pharmacy*, 2013, **39**:704 [Crossref], [Google Scholar], [Publisher]
[35]. Shafiei M., Jafarizadeh-Malmiri H., Rezaei M., Biological activities of chitosan and prepared chitosan-tripolyphosphate nanoparticles using ionic gelation method against various pathogenic bacteria and fungi strains, *Biologia*, 2019, **74**:1561 [Crossref], [Google Scholar], [Publisher]
[36]. Dai T., Tanaka M., Huang Y.Y., Hamblin M.R., Chitosan preparations for wounds and burns: antimicrobial and wound-healing effects, *Expert Review of Anti-Infective Therapy*, 2011, **9**:857 [Crossref], [Google Scholar], [Publisher]
[37]. Sadeghi M., Heidari B., Crosslinked graft copolymer of methacrylic acid and gelatin as a novel hydrogel with pH-responsiveness properties, *Materials*, 2011, **4**:543 [Crossref], [Google Scholar], [Publisher]
[38]. Ray M., Pal K., Anis A., Banthia A., Development and characterization of chitosan-based polymeric hydrogel membranes, *Designed Monomers and Polymers*, 2010, **13**:193 [Crossref], [Google Scholar], [Publisher]
[39]. Taaca K.L.M., De Leon M.J.D., Thumanu K., Nakajima H., Chanlek N., Prieto E.I., Vasquez Jr M.R., Probing the structural features of a plasma-treated chitosan-acrylic acid hydrogel, *Colloids and Surfaces A: Physicochemical and Engineering Aspects*, 2022, **637**:128233 [Crossref], [Google Scholar], [Publisher]
[40]. Sharma P.K., Panda A., Pradhan A., Zhang J., Thakkar R., Whang C.H., Repka M.A., Murthy S.N., Solid-state stability issues of drugs in transdermal patch formulations, *AAPS PharmSciTech*, 2018, **19**:27 [Crossref], [Google Scholar], [Publisher]

HOW TO CITE THIS ARTICLE
Sidhavatam Harshavardhan Reddy, Manimaran V. Formulation and Development of Doxycycline Hyclate Loaded Chitosan Nanoparticles Crosslinked Topical Hydrogel Patches for Healing Diabetic Foot Ulcer. *J. Med. Chem. Sci.*, 2024, 7(6) 753-776.
DOI: https://doi.org/10.26655/JMCHEMSCI.2024.6.1
URL: https://www.jmchemsci.com/article_194566.html